Gene deletion of inositol hexakisphosphate kinase 1 reveals inositol pyrophosphate regulation of insulin secretion, growth, and spermiogenesis

Rashna Bhandari*, Krishna R. Juluri*, Adam C. Resnick†, and Solomon H. Snyder*‡§¶

*The Solomon H. Snyder Department of Neuroscience and Departments of ‡Pharmacology and Molecular Sciences and §Psychiatry and Behavioral Sciences, Johns Hopkins University School of Medicine, 725 North Wolfe Street, Baltimore, MD 21205; and †Division of Neurosurgery at the Children's Hospital of Philadelphia, Department of Neurosurgery, University of Pennsylvania School of Medicine, Philadelphia, PA 19104

Contributed by Solomon H. Snyder, December 26, 2007 (sent for review December 7, 2007)

Inositol pyrophosphates, also designated inositol diphosphates, possess high-energy β-phosphates that can pyrophosphorylate proteins and regulate various cellular processes. They are formed by a family of inositol hexakisphosphate kinases (IP6Ks). We have created mice with a targeted deletion of IP6K1 in which production of inositol pyrophosphates is markedly diminished. Defects in the mutants indicate important roles for IP6K1 and inositol pyrophosphates in several physiological functions. Male mutant mice are sterile with defects in spermiogenesis. Mutant mice are smaller than wild-type despite normal food intake. The mutants display markedly lower circulating insulin.

inositol phosphate kinase | inositol polyphosphate | knockout mouse

Numerous inositol phosphates regulate biological functions with the best characterized, inositol-1,4,5-trisphosphate (IP_3), releasing intracellular calcium (1). Recent attention has focused on the inositol pyrophosphates, also designated inositol diphosphates, of which the best studied are diphosphoinositol pentakisphosphate [5-PP-I(1,2,3,4,6)P_5, here designated IP_7] and bisdiphosphoinositol tetrakisphosphate ([PP]$_2$-IP_4, IP_8) (2–4). These compounds are synthesized by a family of three inositol hexakisphosphate (IP_6) kinases (IP6Ks) (5–7). Inositol pyrophosphates have been implicated in a variety of physiologic functions including apoptosis (8, 9), endocytosis (10, 11), telomere length maintenance (12, 13), and chemotaxis (14). Additionally, another form of IP_7, tentatively identified as 4/6-PP-IP_5, is formed by the Vip1 enzyme in yeast and is implicated in the regulation of cell morphology, cell growth, and phosphate homeostasis (15, 16). Shears *et al.* have established that the mammalian Vip1 ortholog physiologically synthesizes IP_8, which is involved in osmotic regulation (17, 18). Inositol pyrophosphates may exert their functions in two ways, by binding to proteins or via phosphorylation. IP_7 can directly bind cytosolic proteins, such as the cyclin–cyclin-dependent kinase (CDK)-CDK inhibitor (CKI) complex, required for phosphate homeostasis in yeast (19). IP_7 can also compete with membrane phosphoinositides for binding to phosphoinositide-binding modules such as PH domains, as observed during chemotactic regulation in Dictyostelium (14). In addition, IP_7 physiologically phosphorylates proteins in a nonenzymatic fashion, analogous to S-nitrosylation, whereby the β-phosphate is transferred from IP_7 to previously phosphorylated proteins; hence, IP_7 pyrophosphorylates proteins (20, 21).

The various mammalian IP6Ks serve diverse functions. IP6K2 regulates apoptotic cell death (8, 9, 22, 23). IP6K1 has been implicated in the disposition of insulin and glucose. A putative disruption of the IP6K1 gene has been described in a family with type 2 diabetes (24). Illies *et al.* recently showed that selective depletion of IP6K1 by RNA interference in pancreatic beta cells impairs insulin secretion (25). To elucidate the physiologic role of IP6K1, we created mice with a targeted deletion of the exon encoding the C-terminal catalytic domain. We report that these mice display defects in insulin disposition, spermiogenesis, and growth.

Results and Discussion

We generated mice with a targeted deletion of the coding sequence of IP6K1 exon 6 (Fig. 1*a*). This sequence encodes amino acids 265–433, comprising the C-terminal catalytic domain of the protein. Male and female heterozygous mice carrying the IP6K1 knockout allele, were mated to produce wild-type (IP6K1$^{+/+}$) and IP6K1 knockout (IP6K1$^{-/-}$) littermates. RT-PCR analysis of tissues from IP6K1$^{-/-}$ mice, using primers flanking exons 5 and 6, reveals loss of transcript in this region (Fig. 1*b*). As a control, we observe that the analogous region of mRNA encoding IP6K2 is preserved. Protein sequence comparison of IP6K1 with IP_3 3-kinase A and inositol polyphosphate multikinase (IPMK), two other members of the IP kinase family whose crystal structures have been resolved (26–28), indicates that exon 6 encodes the C-terminal subdomain of IP6K1, which is required for ATP binding and catalytic activity. By inference, if the remainder IP6K1 mRNA (exons 1–5) is transcribed and stable, the resulting truncated form of IP6K1 would not possess any catalytic activity.

The relative importance of the three IP_6 kinases in generating IP_7 in different tissues has not been well characterized. We monitored the conversion of [^{3}H]IP_6 to IP_7 and IP_8 in extracts of mouse embryonic fibroblasts (MEFs) prepared from IP6K1 mutant and wild-type embryos (Fig. 1*c*). In whole cell and cytosolic extracts, IP_7 and IP_8 formation are virtually undetectable in the knockout MEFs, whereas a major decrease is evident in nuclear extracts. In intact MEFs we also observed a marked diminution of IP_7 levels after incubation of the cells with [^{3}H]inositol (Fig. 1*d*). Thus, in MEF cell lines, IP6K1 is the predominant source of IP_7 synthesis.

Mating studies reveal a major abnormality in male fertility (Table 1). No pregnancies emerge when homozygous knockout males are mated with wild-type or homozygous knockout females. However, normal rates of pregnancy and litter size are observed when the same females are paired with heterozygous males, suggesting that oogenesis is normal in IP6K1 knockout females. Offspring from wild-type, heterozygous, or knockout females paired with heterozygous males follow expected Mendelian ratios of inheritance (data not shown). Histologic examination of the testes and epididymis of IP6K1$^{-/-}$ males reveals very few advanced spermatids in the seminiferous tubules and no sperm in the epididymis (Fig. 2). Thus, IP6K1 evidently plays an important role in spermiogenesis, the final stage of spermatogenesis during which round spermatids develop into mature, motile spermatozoa.

Author contributions: R.B. and K.R.J. contributed equally to this work; R.B., K.R.J., A.C.R., and S.H.S. designed research; R.B. and K.R.J. performed research; R.B., K.R.J., A.C.R., and S.H.S. analyzed data; and R.B. and S.H.S. wrote the paper.

The authors declare no conflict of interest.

¶To whom correspondence should be addressed at: 725 North Wolfe Street, WBSB 813, Baltimore, MD 21205. E-mail: ssnyder@jhmi.edu.

This article contains supporting information online at www.pnas.org/cgi/content/full/0712227105/DC1.

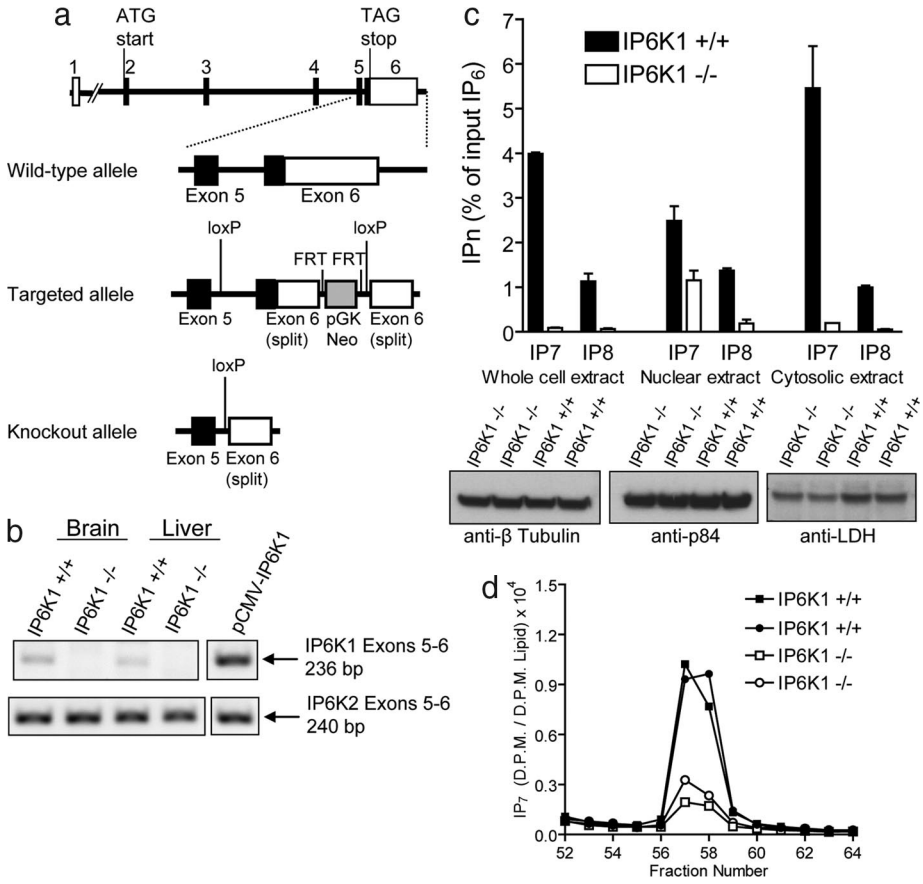

Fig. 1. Generation and characterization of IP6K1 knockout mice. (*a*) Schematic representation of the mouse IP6K1 gene (Ihpk1) with coding regions shaded black, noncoding regions in white, and the exon number indicated on top. A close-up view of exons 5 and 6 in the wild-type, targeted and knockout alleles is shown. The knockout allele loses the splice site, coding region, and a portion of the 3′UTR of exon 6. (*b*) RT-PCR analysis of tissues from wild-type and IP6K1 knockout adult male mice. For both IP6K1 and IP6K2, the forward PCR primer was directed against exon 5 and the reverse primer against the coding region of exon 6. IP6K1 and IP6K2 cDNA in expression plasmids (pCMV) were used as positive controls. (*c*) (*Upper*) IP_6 kinase activity was assayed in extracts prepared from MEFs. Products (IP_7 and IP_8) derived from IP_6 are expressed as a percentage of IP_6 added to the reaction mix. Data are expressed as mean ± SE of duplicate determinations from two cell lines of each genotype. (*Lower*) To ensure that equal amounts of total protein were used for IP_6 kinase assays, the whole cell, nuclear, and cytosolic MEF extracts were quantified by Western blotting with the indicated antibodies. (*d*) IP_7 levels present in two MEF cell lines of each genotype were determined by equilibrium labeling with [^{3}H]inositol and resolution of labeled inositol phosphates by HPLC. The HPLC fractions encompassing the IP_7 peak are shown. Levels of IP_7 in each cell line were normalized against the amount of [^{3}H]inositol incorporated into the lipid fraction.

Male mutant mice are smaller than wild-type with a 15–20% reduction in weight evident consistently from 4 to 10 weeks (Fig. 3*a*) and up to 5 months (data not shown), despite normal food intake (Fig. 3*b*). Female knockout mice also display decreased body weight compared with their wild-type littermates (data not shown). We monitored plasma growth hormone levels, which are the same in mutant and wild-type mice (data not shown).

Because of prior evidence implicating inositol pyrophosphates in insulin disposition, we monitored plasma insulin and detected a striking 65–70% reduction in the mutant mice (Fig. 3*c*). This data correlates with the observations of Illies *et al.* (25) that RNA silencing of IP6K1 in pancreatic beta cells inhibits exocytosis of insulin-containing granules from the readily releasable pool. There-

Table 1. IP6K1 knockout male mice are sterile, whereas females are fertile*

Genotype			
Male	Female	Rate of pregnancy	Litter size
−/−	+/+	0/5	0
−/−	−/−	0/5	0
+/−	+/+	4/5	8.8 ± 1
+/−	−/−	4/5	7.8 ± 0.9
+/−	+/−	7/12	8.5 ± 1

*Three-month-old males and females of the specified genotype were paired for 7 days. The number of pregnant females and the number of pups in each litter were counted. Litter sizes are expressed as mean ± SE for each female.

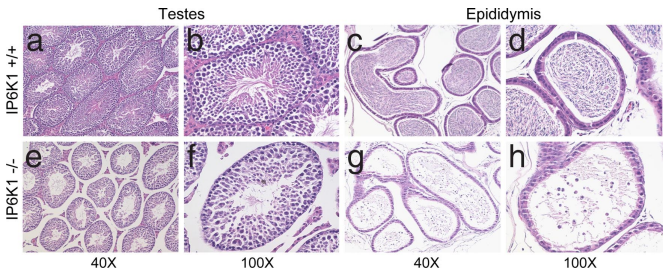

Fig. 2. Spermiogenesis is impaired in male mice lacking IP6K1. Histological analysis of testes and epididymides from wild-type and IP6K1 knockout adult male mice are shown. Cross-sections of the testes [wild-type (*a* and *b*) and knockout (*e* and *f*)] and epididymides [wild-type (*c* and *d*) and knockout (*g* and *h*)] were imaged at ×40 and ×100 magnification as indicated.

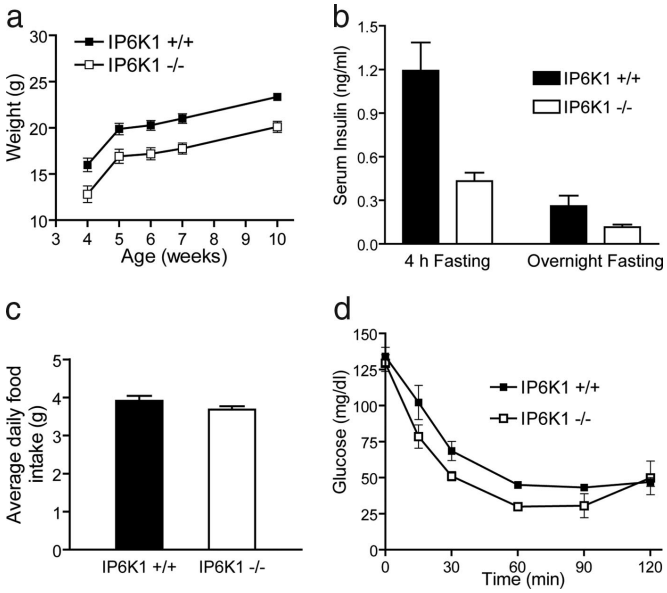

Fig. 3. IP6K1 knockout mice display growth retardation and altered insulin disposition. (*a*) The body weight of wild-type and IP6K1 knockout male littermates, measured once per week, is expressed as mean ± SE ($n = 6–8$). Two-way ANOVA shows significant difference between curves, $P < 0.01$. (*b*) The average daily food intake of 6-week-old male mice is expressed as mean ± SE ($n = 6–8$). There is no significant difference in food intake between wild-type and knockout mice (Student's *t* test, $P > 0.1$). (*c*) Serum insulin levels were measured in wild-type and IP6K1 knockout adult male mice, either after fasting for 4 or 16 h (overnight). Data are mean ± SE ($n = 5–10$). (*d*) Insulin tolerance test was performed by 0.75 unit/kg body weight i.p. insulin injection in adult male mice. Data are mean ± SE ($n = 4$). Two-way ANOVA indicates that the curves for insulin tolerance are significantly different ($P < 0.05$) between IP6K1 knockout and wild-type mice.

fore, loss of IP6K1 in mice most likely lowers insulin secretion from pancreatic beta cells and consequently lowers the levels of circulating insulin.

Because long-term deficiency of insulin might elicit supersensitivity of the insulin-response system, we evaluated insulin tolerance (Fig. 3*d*). The mutant mice display a greater diminution of blood glucose levels in response to insulin than wild-type mice, consistent with higher glucose uptake by tissues in response to insulin.

We wondered whether the apparent supersensitivity to insulin compensates for the impaired insulin secretion and, so, monitored blood glucose, glucose tolerance, and levels of glycosylated hemoglobin (Fig. 4). Mutant mice display normal blood glucose levels whether fed or fasted, manifest a normal glucose tolerance curve, and have normal levels of glycosylated hemoglobin.

How might the phenotypic abnormalities observed in the mutant mice relate to the known functions of IP6K1? Inositol pyrophosphates have been implicated in processes that regulate general metabolism, protein synthesis, cell growth, and cell death. Thus, IP_7 regulates telomere elongation (12, 13), several targets of IP_7 pyrophosphorylation participate in ribosomal biogenesis (4, 21), IP_7 levels fluctuate during the cell cycle (29), and IP6K2 plays a prominent role in apoptotic cell death (8, 9). Some of these actions may be relevant to the phenotype we have observed. There is abundant evidence for a role of IP_7 in vesicular trafficking. Yeast with deletion of IP6K manifests striking defects in vesicular endocytosis and vacuolar morphology (10, 11, 30). Clathrin-associated proteins that regulate endocytosis and exocytosis bind IP_6 and IP_7 with selective high affinity (11, 31, 32). The β3 subunit of the adaptor protein AP3 is pyrophosphorylated by IP_7 (20). The abnormalities of the IP6K1 mutant mice may be related to processes in which vesicular secretion is prominent. Insulin release occurs directly through vesicular secretion. The defects in spermiogenesis could result from multiple factors, including vesicular trafficking events or the secretion of regulatory endocrine and paracrine factors (33–35). We do not have insights into the molecular mechanisms underlying the growth defects of the mutant mice, but insulin itself participates in growth dynamics, and impairment of insulin secretion can lead to growth deficiency (36). Disruption of components of the insulin-signaling pathway can result in infertility and growth retardation (37–39). Defects in insulin secretion after IP6K1 deletion may be linked to the regulation of Ca^{2+}-dependent activator protein for secretion (CAPS), a protein required for Ca^{2+}-triggered exocytosis of insulin (40) and which possesses motifs for IP_7-mediated pyrophosphorylation.

In summary, the phenotype of IP6K1-deleted mice establishes that cellular actions of inositol pyrophosphates, including regulation of vesicular trafficking, impact organismic functions such as hormonal disposition, growth, and fertility.

Materials and Methods

Generation and Maintenance of IP6K1 Knockout Mice. The gene encoding mouse IP6K1, *Ihpk1*, is located on chromosome 9 and has 6 exons, of which exon 1 is exclusively noncoding (Fig. 1*a*). The start codon is located in exon 2, and the stop codon is located in exon 6. Exon 6 is composed of 3,318 bp, of which the first 510 bp encode the C-terminal region of IP6K1 (amino acids 265–433), and the remaining 2,808 bp give rise to the 3′ untranslated region (UTR) of the mRNA. Our strategy was to delete the coding region of exon 6, including the exon 6 splice site. The resulting transcript would lack exon 6 (including the 3′UTR) and therefore be unstable, resulting in a complete knockout. Alternatively, cryptic splicing may occur between exon 5 and the remainder of exon 6, possibly generating a stable mRNA lacking the exon 6 coding sequence, resulting in a catalytically inactive, truncated protein lacking the C-terminal subdomain.

IP6K1$^{+/-}$ mice were generated at Ozgene. The targeting construct was based

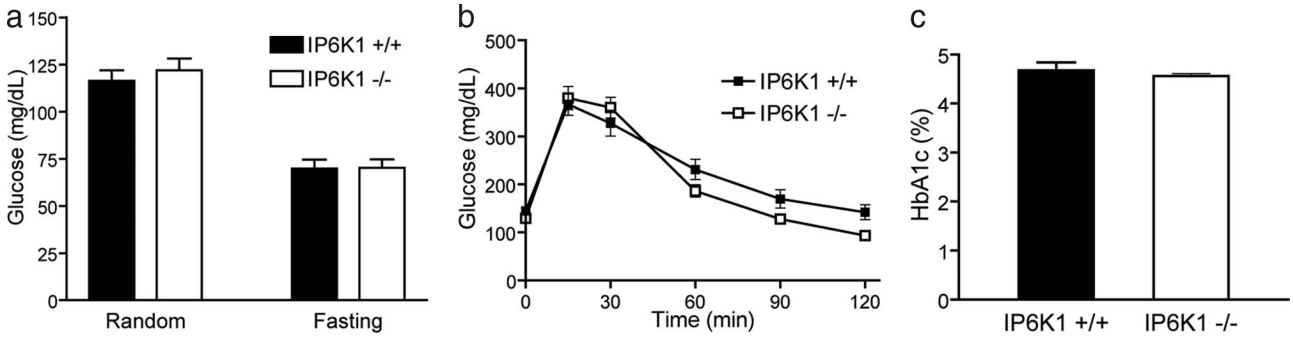

Fig. 4. Mice lacking IP6K1 are not diabetic despite low insulin levels. (*a*) Tail vein blood glucose measured in ad libitum-fed or 16-hour-fasted adult male mice. Data are mean ± SE ($n = 7$ or 8). (*b*) Glucose tolerance test by 2 g/kg body weight i.p. glucose injection in adult male mice. Data are mean ± SE ($n = 6$ or 7). (*c*) Measurement of glycosylated hemoglobin (HbA1c) in whole blood from adult male and female mice. Data are mean ± SE ($n = 5$).

on the sequence of the C57BL/6 strain *Ihpk1* gene (Ensembl gene ID: ENSMUSG00000032594). A LoxP site was inserted between exons 5 and 6, 295 bp upstream of the exon 6 splice site. A phosphoglycerine kinase (PGK) Neo cassette flanked by FLP recombinase target (FRT) sequences and another LoxP site was inserted 1,464 bp downstream of the stop codon in exon 6. The targeting vector was electroporated into 129SV/J ES cells, and Neomycin resistant ES cells were microinjected into C57BL/6 blastocysts and implanted into pesudo-pregnant female mice. The resulting chimeric mice were crossed with knockin C57BL/6 mice carrying Cre recombinase driven by a PGK promoter to generate heterozygous mice carrying the IP6K1 knockout allele and Cre recombinase (IP6K1$^{+/-}$/*Cre*). These mice were interbred and F_1 heterozygous mice lacking *Cre* (IP6K1$^{+/-}$) were subsequently interbred to generate wild-type (IP6K1$^{+/+}$) and IP6K1 knockout (IP6K1$^{-/-}$) littermates used for phenotypic and metabolic studies.

All mice were maintained on a 129SV-C57BL/6 mixed background. Animal care and experimentations were approved by the Johns Hopkins University Animal Care and Use Committee. Mice were housed in a 12-h light/12-h dark cycle, at an ambient temperature of 22°C, and fed standard rodent chow.

Genotyping and RT-PCR Analysis. Mice were genotyped by PCR analysis of genomic DNA from tail biopsies. The detailed genotyping strategy is described in the supporting information (SI) *Materials and Methods*.

RT-PCR analysis was used to assess whether the IP6K1 transcript was missing in the knockout mice. RNA was prepared from tissues obtained from IP6K1 knockout mice and their wild-type littermates by using TRIZOL reagent (Invitrogen). cDNA was prepared by using Oligo(dT) primers (Invitrogen) and the Omniscript reverse transcriptase kit (Qiagen). PCR was performed by using cDNA templates and primers flanking exons 5 and 6 of IP6K1 (see SI Fig. 5). IP6K2 primers were used as a positive control to assess the quality of cDNA.

Generation of MEF Cell Lines. Wild-type (IP6K1$^{+/+}$) and mutant (IP6K1$^{-/-}$) E14 embryos were isolated from a single heterozygous female that had been paired with a heterozygous male. The head and organs were removed, and the remaining carcasses were minced and incubated in trypsin to obtain single cells. These primary fibroblasts were transfected with a plasmid encoding the SV40 Large T antigen (Addgene plasmid 9053: pSG5 Large T), and passaged five times at split ratios of 1:10 to yield independent, immortalized MEF cell lines obtained from separate embryos. Two cell lines of each genotype (IP6K1$^{+/+}$ and IP6K1$^{-/-}$) were used for experiments. Cells were cultured in DMEM (Invitrogen) supplemented with 10% FBS (Gemini Bio-Products), L-glutamine (2 mM; Invitrogen), and penicillin (100 units/ml)/streptomycin (100 μg/ml) (Invitrogen).

Measurement of IP_6 Kinase Activity. Extracts were prepared from MEFs by sonication in the presence of 50 mM Hepes (pH 7.4), 150 mM NaCl, 1 mM EDTA, 1 mM DTT, 1% Triton X-100, protein phosphatase inhibitor mixture (Sigma), and protease inhibitor mixture (Sigma). Nuclear and cytosolic fractions from MEFs were obtained by using a nuclear/cytosol fractionation kit (BioVision). Protein content in the extracts was quantified by using the Bradford assay.

Whole cell, nuclear, or cytosolic extracts were used in an IP_6 kinase activity assay. Extracts (35 μg total protein) were incubated in assay buffer [20 mM Tris·HCl (pH 7.4), 6 mM $MgCl_2$, 1 mM DTT], in the presence of [^{3}H]IP_6 (100 μM, 150,000 dpm, Perkin–Elmer Life Sciences), ATP (5 mM), Creatine kinase (40 units/ml), and phosphocreatine (10 mM), at 37°C for 1 h. Assays were terminated by the addition of Na_2EDTA (5 mM), followed by perchloric acid (0.6 M), and quenched as described previously (2). [^{3}H]IP_6 and its products, [^{3}H]IP_7 and [^{3}H]IP_8, were resolved by HPLC with a Partisphere SAX column (Whatman), with a gradient generated by mixing Buffer A (1 mM Na_2EDTA) and Buffer B [Buffer A plus 1.3 M $(NH_4)_2HPO_4$ (pH 3.85)] as follows: 0–5 min, 0% B; 5–10 min, 0–30% B; 10–60 min, 30–100% B; 60–75 min, 100% B. One-milliliter fractions were collected, and the radiolabeled fractions were identified by using a liquid scintillation counter. When comparing IP_6 kinase activity from extracts prepared from different cell lines, total, nuclear, or cytoplasmic protein content was normalized by Western blotting by using antibodies against β-tubulin (Upstate Biotechnology), p84/N5 (GeneTex), or lactate dehydrogenase (Chemicon International), respectively.

Analysis of Inositol Phosphate Content in Cells. MEFs were plated at a density of 2×10^6 cells per 10-cm dish, then labeled with 200 μCi (1 Ci = 37 GBq) [^{3}H]inositol (Perkin–Elmer Life Sciences) for 5 days. Soluble inositol phosphates were extracted from labeled cells as described previously (41). Inositol incorporated into lipids was measured by extracting the remaining cell pellet with 0.1 M NaOH, 0.1% Triton X-100 overnight at room temperature with shaking and counting a fraction of the solubilized material in a liquid scintillation counter. The [^{3}H]-labeled inositol phosphates were resolved by HPLC as described above. Soluble inositol phosphate levels were normalized against total lipid inositol content for each cell line.

Phenotypic Analysis of Mice. Histological analysis of the testes and epididymis was performed by the Phenotyping Core in the Department of Molecular and Comparative Pathobiology, Johns Hopkins University. Eleven-week-old male mice (IP6K1$^{+/+}$ and IP6K1$^{-/-}$ littermates) were killed with carbon dioxide, and the dissected tissue specimens were fixed in 10% neutral buffered formalin for 24 h before trimming for histology processing. Paraffin-embedded tissue sections were stained with hematoxylin/eosin according to standard protocols.

To monitor weight gain, male mice (n = 6–8) were weighed once per week. To measure daily food intake, singly housed, 6-week-old male mice were given a preweighed amount of rodent chow (150 g), and the remaining food (to the nearest 0.1 g) was weighed once a day, at 1500 h, for the next 3 days. The average amount of food consumed per mouse per day was calculated as mean ± SE (n = 6–8). The mice drank water ad libitum throughout the study.

Metabolic Analysis. To measure serum insulin levels, blood was collected by facial vein puncture from 4- to 6-month-old male mice (n = 5–10), after they were starved either for 4 h or overnight (16 h). Serum was obtained by centrifugation at 10,000 × g for 10 min at 4°C, and insulin levels were measured by using the Insulin (Mouse) Ultrasensitive EIA kit (Aplco Diagnostics). Glycosylated hemoglobin (HbA1c) levels were measured in whole blood collected in K_2EDTA-coated tubes by facial vein puncture from 4- to 6-month-old male and female mice by using the A1CNow$^+$ monitor (Metrika).

Blood glucose levels were measured from tail vein bleeding of overnight (16 h) fasted or ad libitum-fed 5 month old male mice (n = 7 to 8) by using an Ascensia Contour blood glucose meter and test strips (Bayer). For glucose tolerance tests, mice were fasted for 4–6 h and injected i.p. with 2 g/kg body weight glucose. Blood glucose was measured at 0, 15, 30, 60, 90, and 120 min by tail vein bleeding. For insulin tolerance tests, mice were fasted for 4 h and were given 0.75 units/kg body weight human regular insulin (Sigma) i.p. Blood glucose measurements were obtained from tail veins at 0, 15, 30, 60, 90, and 120 min postinjection.

Statistics. The data are presented as mean ± SEM. All statistical analyses were performed by using GraphPad Prism. Differences between two groups were assessed by unpaired Student's t test. Multiple parameters were analyzed by ANOVA test. $P < 0.05$ was considered significant.

ACKNOWLEDGMENTS. We thank Adolfo Saiardi and the Ozgene team for design and construction of the IP6K1 knockout mouse; the following persons for valuable discussions and suggestions with regard to characterization of the knockout mice: Franz Matschinsky and Nicolai Doliba for metabolic analysis; Cory Brayton, Teresa Southard, Nadine Forbes and Craig Morrell for phenotypic and histologic analysis; Barry Zirkin and Bill Wright for analysis of spermatogenesis; William Hahn for the SV40 Large T antigen carrying plasmid; Tom Martin and Chris Barker for helpful discussions on insulin exocytosis; and Adele Snowman, Bingnan Kang, Masoumeh Saleh, David Maag, Sangwon Kim, Tom Sedlak, Alex Huang, and Raghunand Tirumalai for assistance and helpful suggestions. A.C.R. is supported by the Division of Neurosurgery at the Children's Hospital of Philadelphia. This work was supported by U.S. Public Health Service Grant MH18501 and Research Scientist Award DA00074 (to S.H.S.).

1. Berridge MJ, Lipp P, Bootman MD (2000) The versatility and universality of calcium signalling. *Nat Rev Mol Cell Biol* 1:11–21.
2. Menniti FS, Miller RN, Putney JW, Jr, Shears SB (1993) Turnover of inositol polyphosphate pyrophosphates in pancreatoma cells. *J Biol Chem* 268:3850–3856.
3. Stephens L, *et al.* (1993) The detection, purification, structural characterization, and metabolism of diphosphoinositol pentakisphosphate(s) and bisdiphosphoinositol tetrakisphosphate(s). *J Biol Chem* 268:4009–4015.
4. Bennett M, Onnebo SM, Azevedo C, Saiardi A (2006) Inositol pyrophosphates: Metabolism and signaling. *Cell Mol Life Sci* 63:552–564.
5. Saiardi A, *et al.* (1999) Synthesis of diphosphoinositol pentakisphosphate by a newly identified family of higher inositol polyphosphate kinases. *Curr Biol* 9:1323–1326.
6. Saiardi A, *et al.* (2001) Identification and characterization of a novel inositol hexakisphosphate kinase. *J Biol Chem* 276:39179–39185.
7. Schell MJ, *et al.* (1999) PiUS (Pi uptake stimulator) is an inositol hexakisphosphate kinase FEBS. *Lett* 461:169–172.
8. Morrison BH, Bauer JA, Kalvakolanu DV, Lindner DJ (2001) Inositol hexakisphosphate kinase 2 mediates growth suppressive and apoptotic effects of interferon-beta in ovarian carcinoma cells. *J Biol Chem* 276:24965–24970.
9. Nagata E, *et al.* (2005) Inositol hexakisphosphate kinase-2, a physiologic mediator of cell death. *J Biol Chem* 280:1634–1640.
10. Dubois E, *et al.* (2002) In Saccharomyces cerevisiae, the inositol polyphosphate kinase activity of Kcs1p is required for resistance to salt stress, cell wall integrity, and vacuolar morphogenesis. *J Biol Chem* 277:23755–23763.
11. Saiardi A, *et al.* (2002) Inositol pyrophosphates regulate endocytic trafficking. *Proc Natl Acad Sci USA* 99:14206–14211.

12. York SJ, *et al.* (2005) Inositol diphosphate signaling regulates telomere length. *J Biol Chem* 280:4264–4269.
13. Saiardi A, *et al.* (2005) Inositol pyrophosphates regulate cell death and telomere length through phosphoinositide 3-kinase-related protein kinases. *Proc Natl Acad Sci USA* 102:1911–1914.
14. Luo HR, *et al.* (2003) Inositol pyrophosphates mediate chemotaxis in Dictyostelium via pleckstrin homology domain-PtdIns(3,4,5)P3 interactions. *Cell* 114:559–572.
15. Mulugu S, *et al.* (2007) A conserved family of enzymes that phosphorylate inositol hexakisphosphate. *Science* 316:106–109.
16. Lee YS, Mulugu S, York JD, O'Shea EK (2007) Regulation of a cyclin-CDK-CDK inhibitor complex by inositol pyrophosphates. *Science* 316:109–112.
17. Choi JH, *et al.* (2007) Purification, sequencing, and molecular identification of a mammalian PP-InsP5 kinase that is activated when cells are exposed to hyperosmotic stress. *J Biol Chem* 282:30763–30775.
18. Pesesse X, Choi K, Zhang T, Shears SB (2004) Signaling by higher inositol polyphosphates. Synthesis of bisdiphosphoinositol tetrakisphosphate (''InsP8'') is selectively activated by hyperosmotic stress. *J Biol Chem* 279:43378–43381.
19. Lee YS, Huang K, Quiocho FA, O'Shea EK (2008) Molecular basis of cyclin-CDK-CKI regulation by reversible binding of an inositol pyrophosphate. *Nat Chem Biol* 4:25–32.
20. Saiardi A, *et al.* (2004) Phosphorylation of proteins by inositol pyrophosphates. *Science* 306:2101–2105.
21. Bhandari R, *et al.* (2007) Protein pyrophosphorylation by inositol pyrophosphates is a posttranslational event. *Proc Natl Acad Sci USA* 104:15305–15310.
22. Morrison BH, *et al.* (2002) Inositol hexakisphosphate kinase 2 sensitizes ovarian carcinoma cells to multiple cancer therapeutics. *Oncogene* 21:1882–1889.
23. Morrison BH, *et al.* (2005) Apo2L/TRAIL induction and nuclear translocation of inositol hexakisphosphate kinase 2 during IFN-beta-induced apoptosis in ovarian carcinoma. *Biochem J* 385:595–603.
24. Kamimura J, *et al.* (2004) The IHPK1 gene is disrupted at the 3p21.31 breakpoint of t(3;9) in a family with type 2 diabetes mellitus. *J Hum Genet* 49:360–365.
25. Illies C, *et al.* (2007) Requirement of inositol pyrophosphates for full exocytotic capacity in pancreatic cells. *Science* 318:1299–1302.
26. Gonzalez B, *et al.* (2004) Structure of a human inositol 1,4,5-trisphosphate 3-kinase: substrate binding reveals why it is not a phosphoinositide 3-kinase. *Mol Cell* 15:689–701.
27. Miller GJ, Hurley JH (2004) Crystal structure of the catalytic core of inositol 1,4,5-trisphosphate 3-kinase. *Mol Cell* 15:703–711.
28. Holmes W, Jogl G (2006) Crystal structure of inositol phosphate multikinase 2 and implications for substrate specificity. *J Biol Chem* 281:38109–38116.
29. Barker CJ, *et al.* (2004) Complex changes in cellular inositol phosphate complement accompany transit through the cell cycle. *Biochem J* 380:465–473.
30. Saiardi A, Caffrey JJ, Snyder SH, Shears SB (2000) The inositol hexakisphosphate kinase family. Catalytic flexibility and function in yeast vacuole biogenesis. *J Biol Chem* 275:24686–24692.
31. Ye W, *et al.* (1995) Inhibition of clathrin assembly by high affinity binding of specific inositol polyphosphates to the synapse-specific clathrin assembly protein AP-3. *J Biol Chem* 270:1564–1568.
32. Voglmaier SM, *et al.* (1992) Inositol hexakisphosphate receptor identified as the clathrin assembly protein AP-2. *Biochem Biophys Res Commun* 187:158–163.
33. McLachlan RI, *et al.* (2002) Identification of specific sites of hormonal regulation in spermatogenesis in rats, monkeys, and man Recent. *Prog Horm Res* 57:149–179.
34. Huhtaniemi I, Bartke A (2001) Perspective: Male reproduction. *Endocrinology* 142:2178–2183.
35. Moreno RD, *et al.* (2000) Vesicular traffic and golgi apparatus dynamics during mammalian spermatogenesis: Implications for acrosome architecture. *Biol Reprod* 63:89–98.
36. Duvillie B, *et al.* (1997) Phenotypic alterations in insulin-deficient mutant mice. *Proc Natl Acad Sci USA* 94:5137–5140.
37. Rane SG, *et al.* (1999) Loss of Cdk4 expression causes insulin-deficient diabetes and Cdk4 activation results in β-islet cell hyperplasia. *Nat Genet* 22:44–52.
38. Bruning JC, *et al.* (2000) Role of brain insulin receptor in control of body weight and reproduction. *Science* 289:2122–2125.
39. Froment P, *et al.* (2004) Reproductive abnormalities in human insulin-like growth factor-binding protein-1 transgenic male mice. *Endocrinology* 145:2080–2091.
40. Waselle L, *et al.* (2005) Role of phosphoinositide signaling in the control of insulin exocytosis. *Mol Endocrinol* 19:3097–3106.
41. Azevedo C, Saiardi A (2006) Extraction and analysis of soluble inositol polyphosphates from yeast. *Nat Protoc* 1:2416–2422.